

ACCEPTED MANUSCRIPT

Signal conditioning using logarithmic amplifier for biomedical applications of EIT

To cite this article before publication: Mukta Saxena *et al* 2020 *Physiol. Meas.* in press <https://doi.org/10.1088/1361-6579/abc1b4>

Manuscript version: Accepted Manuscript

Accepted Manuscript is “the version of the article accepted for publication including all changes made as a result of the peer review process, and which may also include the addition to the article by IOP Publishing of a header, an article ID, a cover sheet and/or an ‘Accepted Manuscript’ watermark, but excluding any other editing, typesetting or other changes made by IOP Publishing and/or its licensors”

This Accepted Manuscript is © 2020 Institute of Physics and Engineering in Medicine.

During the embargo period (the 12 month period from the publication of the Version of Record of this article), the Accepted Manuscript is fully protected by copyright and cannot be reused or reposted elsewhere.

As the Version of Record of this article is going to be / has been published on a subscription basis, this Accepted Manuscript is available for reuse under a CC BY-NC-ND 3.0 licence after the 12 month embargo period.

After the embargo period, everyone is permitted to use copy and redistribute this article for non-commercial purposes only, provided that they adhere to all the terms of the licence <https://creativecommons.org/licenses/by-nc-nd/3.0>

Although reasonable endeavours have been taken to obtain all necessary permissions from third parties to include their copyrighted content within this article, their full citation and copyright line may not be present in this Accepted Manuscript version. Before using any content from this article, please refer to the Version of Record on IOPscience once published for full citation and copyright details, as permissions will likely be required. All third party content is fully copyright protected, unless specifically stated otherwise in the figure caption in the Version of Record.

View the [article online](#) for updates and enhancements.

Signal conditioning using Logarithmic Amplifier for biomedical applications of EIT

Mukta Saxena¹, D C Gharpure¹ and V G Wagh²

¹Department of Electronic Science, Savitribai Phule Pune University, Pune, Maharashtra, India

²V N Naik College, Nashik, Pune, Maharashtra, India

E-mail: muktavrm@gmail.com

Received xxxxxx

Accepted for publication xxxxxx

Published xxxxxx

Abstract. *Objective:* The aim of this study was to explore the use of a logarithmic amplifier to improve the spatial resolution of a low-cost Electrical Impedance Tomography (EIT) system. In an EIT system, the measured signal has a large dynamic range from μV to mV , which requires high resolution ADC cards. Logarithmic amplifier reduces the dynamic range, by expanding lower values and compressing higher values, thereby improving the sensitivity and at the same time preventing signal from saturation. In addition, a low resolution ADC can be used, making the system cost effective. This work evaluates the performance of a logarithmic amplifier and a linear amplifier used for signal conditioning, in a low-cost EIT system. *Approach:* Two EIT systems based on linear amplifier and logarithmic amplifier were designed. Phantom experiments were carried out with very small amounts of current injection. The signal-to-noise ratio (SNR), image quality, minimum detectable size and minimum detectable conductivity change were obtained. *Main Results:* Logarithmic amplifier based EIT system increased the average SNR by 4dB. It also showed improvement in resolution (RES) and contrast-to-noise ratio (CNR) of the images. Minimum size detectable by the logarithmic amplifier based system was of radius 0.25 cm in a tank of radius 11cm and the minimum change in conductivity detectable was 11 %. *Significance:* Logarithmic amplifier based signal conditioning is a promising technique for improving the spatial resolution a low-cost EIT system that has a low resolution ADC.

Keywords: Electrical Impedance Tomography, bio imaging, signal processing

1. Introduction

Electrical Impedance Tomography (EIT) is a low-cost and non-invasive technique which has gained tremendous popularity in areas like medical imaging, process control, tissue engineering, biotechnology and many other fields (Barber 2003). EIT images the conductivity variation inside a body using electrodes attached to the surface (Brown 2003). Small value of current is injected through the electrodes attached to the body and surface potentials are measured. Conductivity distribution is estimated from the surface measurements by solving the inverse problem. EIT suffers from low spatial

1
2
3
4
5 resolution due to the ill posed nature of the inverse problem (Holder 2004). This ill
6 posed nature makes the EIT system more sensitive to noise and small measurement
7 errors may lead to larger errors in the reconstruction resulting in image artefacts
8 (Martin and Choi 2017). To stabilize the solution of the inverse problem in presence
9 of noise, regularization is required (Ranade and Damayanti C. Gharpure 2019), (Xu,
10 Bing Han, and Dong 2018). Regularization improves the stability of the solution at
11 the cost of image resolution as the reconstructed images have blurred edges (J. Wang,
12 Bo Han, and W. Wang 2019). In addition, low values of currents result in very weak
13 signals and hence any slight measurement error or noise affects the signal-to-noise ratio
14 (Yu et al. 2014). Due to the poor signal to noise ratio (SNR) of the measured EIT
15 data, a large amount of regularization is required for the reconstruction which reduces
16 the image resolution. By increasing the SNR of the measurement, the sensitivity and
17 the spatial resolution can be improved (Rafiei-Naeini, Wright, and McCann 2007).

18 Small amount of currents are injected in EIT systems owing to safety concerns in
19 case of biomedical applications, which result in the measured signals having smaller
20 values. As we go away from the current injected electrodes, the signals developed on
21 the electrodes decrease and vary in magnitude from μV to mV . Linear amplifiers are
22 used to amplify the signal followed by high resolution ADCs to cover the large dynamic
23 range (Boyle et al. 2019). Some systems also use Programmable Gain Amplifiers
24 (PGA) with adaptive control to prevent signal from saturation and at the same time
25 detect small signals (Takhti, Teng, and Odame 2018). Since both are linear amplifiers,
26 noise is equally amplified with no improvement in the signal-to-noise ratio (SNR) of
27 the system.

28 Logarithmic amplifier compresses larger values and expands lower values reducing
29 the dynamic range of the signal, thereby enabling the use of low-resolution ADC
30 (Reynolds 1965). With the reduced dynamic range, the relative contribution of the
31 expanded smaller values in the reconstruction increases, thereby reducing the artefacts
32 in the reconstruction. This reduces the amount of regularization required resulting
33 in improved image resolution. Another major limitation of EIT is that it is less
34 sensitive to the conductivity change of interest and more sensitive to noise in the
35 measurements (Adler, Grychtol, and Bayford 2015). The poor signal to noise ratio
36 makes the detection of small conductivity contrasts more challenging. Logarithmic
37 amplifier improves the SNR, aiding in detection of small conductivity changes (Verma,
38 D. C. Gharpure, and Wagh 2019).

39 This paper presents the use of a logarithmic amplifier for improving the spatial
40 resolution of an EIT system as well as its sensitivity to small conductivity changes.
41 Owing to the safety concerns in case of biomedical applications, the study was carried
42 out using a very small current of 1 mA. Experiments carried out to obtain SNR of the
43 system, minimum size of the object detectable, image resolution and contrast to noise
44 ratio are detailed. A biological phantom was developed with a cucumber in a saline
45 filled tank to analyze the sensitivity of the EIT system to conductivity change.

46 Recently, EIT is being used for cell imaging applications with the development of
47 micro-technologies (Yin et al. 2018). Since these measurements are at cellular level,
48 the measured signal is very small and more susceptible to noise. The logarithmic
49 amplifier based EIT system is further tested with a mini-EIT sensor developed for cell
50 imaging applications.

51 The study was carried out using a low resolution data acquisition card (NI USB
52 6008, National Instruments Corporation, Austin, TX, USA) with 12-bit ADC. Most
53 of the EIT systems use 16-bit or higher ADCs for high resolution imaging (Bera and
54
55
56
57
58
59
60

Nagaraju 2009). The promising results obtained using the logarithmic amplifier and 12-bit ADC, make the system more cost effective and beneficial, especially for research purposes.

2. Materials and Methods

2.1. EIT Principle

An EIT system comprises electrodes attached to the surface of the body whose conductivity is to be mapped as shown in figure 1.

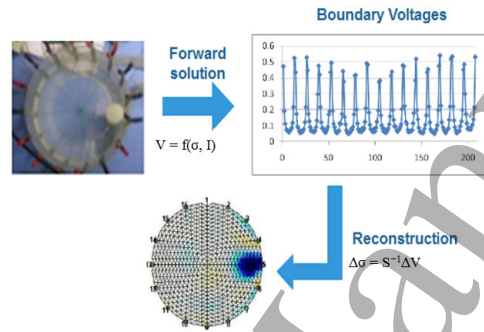


Figure 1: Principle of EIT system

Current is injected through a pair of electrodes and boundary voltages are measured on the remaining pairs of electrodes serially. The measurement protocol used in this paper is based on the adjacent method (Khan and Ling 2019). For each excitation, there are thirteen measurements resulting in 208 voltage values, which are used for reconstruction of the image as shown in figure 1.

In EIT, measured voltages ' V ' are a nonlinear function of conductivity ' σ ' and current ' I ' as (Yu et al. 2014) :

$$V = f(\sigma, I) \quad (1)$$

During reconstruction, the change in conductivity distribution ' $\Delta\sigma$ ' is estimated from the change in boundary voltages ' ΔV ' as:

$$\Delta\sigma = S^{-1}\Delta V \quad (2)$$

where S is the sensitivity matrix related to conductivity change

2.2. Logarithmic amplifier

Logarithmic amplifier will convert linear input voltage to its logarithmic output. Let us assume the signal is represented as:

$$x = s + n \quad (3)$$

where ' s ' is the signal and ' n ' is the noise. Taking logarithm of the signal ' x ' will result in output signal ' y ' expressed as (Verma, D. C. Gharpure, and Wagh 2019):

$$y = \log(s) + \frac{n}{s} - \frac{n^2}{2s^2} + \frac{n^3}{3s^3} + \dots \quad (4)$$

4

According to Equation 4, the noise will be reduced for input signals greater than noise ($s/n > 1$). For signals less than noise ($s/n < 1$), if a bias greater than that of the standard deviation of the noise is given to the signal, logarithmic amplifier improves the SNR (Chen 1969).

Logarithmic amplifier is designed using a general purpose operational amplifier (OP07, analog devices, USA) with a diode in the feedback circuit as shown in figure 2. Positive Voltage 'Vin' is input through resistance 'R1'. The diode in the circuit is

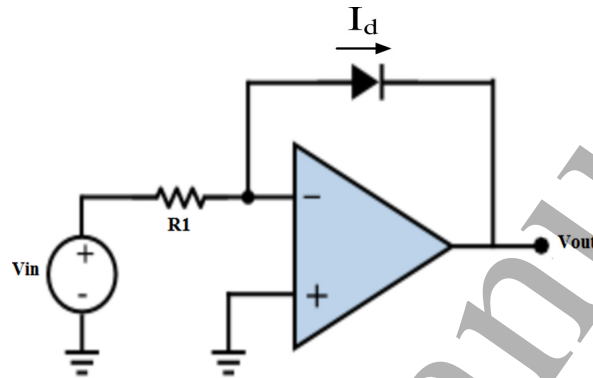


Figure 2: Logarithmic amplifier circuit diagram

forward biased and the current equation of a diode is given as:

$$I_d = I_s(\exp(V/V_t) - 1) \quad (5)$$

where ' I_s ' is the reverse saturation current, ' V ' is voltage across the diode; ' V_t ' is the voltage equivalent of temperature. Applying Kirchoff's current rule at inverting terminal of operational amplifier, we get

$$(0 - V_{in})/R1 + I_d = 0 \quad (6)$$

which implies

$$I_d = V_{in}/R1 \quad (7)$$

Substituting Equation 3 in Equation 5 we get

$$I_s(\exp(V/V_t) - 1) = V_{in}/R1 \quad (8)$$

Since $V \gg V_t$ and $V = -V_{out}$ (negative feedback) Equation 6 reduces to

$$V_{out} = -V_t \ln(V_{in}/(I_s R1)) \quad (9)$$

According to Equation 9, the input voltage is converted to its logarithmic output.

2.3. Logarithmic amplifier based EIT system.

The block diagram of the logarithmic amplifier based Electrical Impedance Tomography system is shown in figure 3. A constant current source with grounded load is developed based on the Howland topology (Bera and Jampana 2010). Adjacent

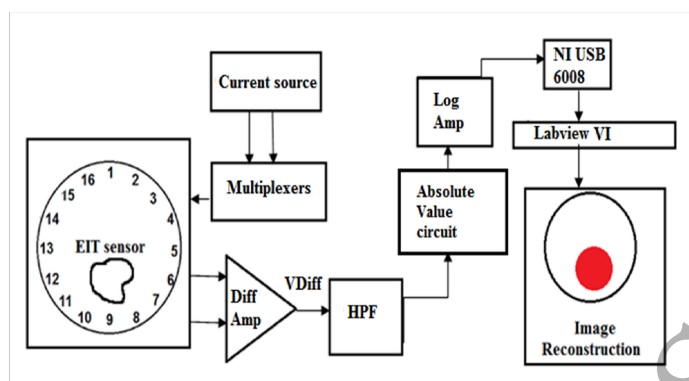


Figure 3: Block diagram for logarithmic amplifier based EIT system

measurement protocol is used, where current is injected through a pair of electrodes and voltages are measured on the remaining pairs of electrodes. Four Analog Multiplexers (ADG506) are used for switching of the electrodes. The voltages developed on the electrodes are fed to a unity gain instrumentation amplifier (INA118) which has a high CMRR of 110dB (INA 118 datasheet). The output signal (VDiff) is then filtered using a high pass filter (HPF) with the cutoff frequency of 1 kHz to eliminate low frequency noise and DC offsets. Since the logarithmic amplifier circuit requires a positive input signal, the filtered signal is fed to the absolute value circuit designed using the AD8606 operational amplifier. The signal is then passed through the logarithmic amplifier. LabVIEW VI is designed to acquire the data using a data acquisition card (NI USB 6008) which has a 12-bit ADC and stores the data in the form of text files.

The complete circuit consisting of the absolute value circuit and the logarithmic amplifier circuit as shown in figure 4a is simulated in a software named Proteus. The circuit consists of three diodes, D5, D2 and D4 (IN4148) and three Resistors R1, R2 and R3 of resistance values 10 Ω , 10 Ω and 1 k Ω . A sinusoidal input signal (V_{in}) of peak to peak voltage 10 mV is applied and the simulated output voltage (V_{out}) has the amplified value of 0.43 V. The inset in figure 4a shows the simulation graph for input signal (V_{in}) represented by blue color and output signal (V_{out}) represented by red color. The input is varied from 10 mV to 1 V. The corresponding simulated output ranging from 0.43V to 0.624V is shown in figure 4b. The non-linear curve in figure 4b shows significant changes for low values of input signal and less variation for higher values. Since the dynamic range is compressed with the logarithmic amplifier, the reference voltage can be reduced accordingly, which improves the resolution of the ADC (Oljaca and Baker 2009). The output is further fed to the linear amplifier.

One of the limitations of the present circuit is its limited input range of 10 mV to 1 V.

2.4. Design of a Linear amplifier based EIT system

For a linear amplifier based EIT system, the filtered signal is amplified using a linear amplifier as shown by the block diagram in figure 5a. Linear amplifier is designed using an operational amplifier (OP07) as shown in figure 5b, where R1 and R2 are resistors and V_{in} is the input sinusoidal voltage. The value for R1 is 1 k Ω and R2 is

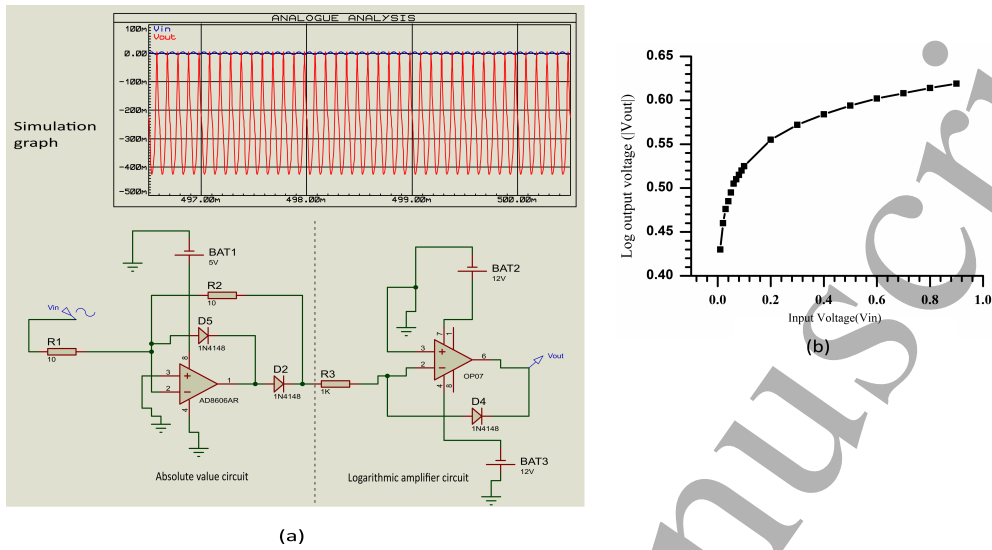


Figure 4: (a) Simulation of Logarithmic amplifier based signal conditioning, (b) Output characteristics

varied to adjust the gain.

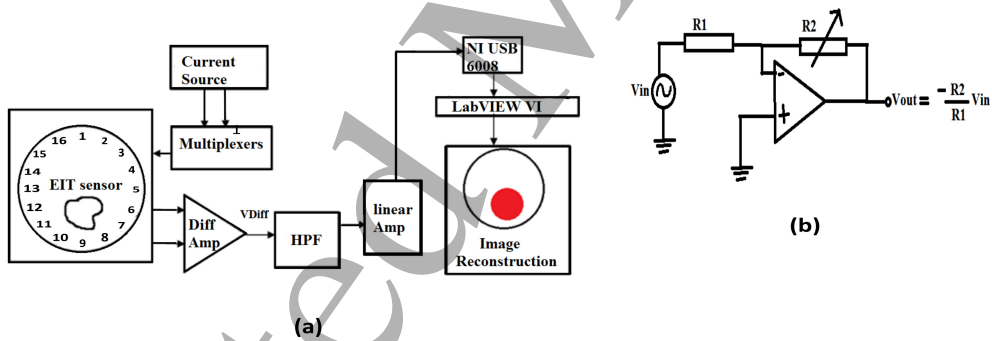


Figure 5: (a) Block diagram for Linear amplifier based EIT system, (b) Linear amplifier design

2.5. Signal-to-noise ratio analysis for linear and logarithmic amplifiers

Input sinusoidal signal of 10 mV (peak-to-peak) with 15 kHz frequency is fed to both linear and logarithmic amplifier and the spectra of output signals are analyzed. Figure 6 shows the spectrum of the output signals from both the circuits obtained using a spectrum analyzer (Tektronix RSA507A) which has a frequency range of 9 kHz to 7.5 GHz.

The spectrum shows that the noise floor of the linear amplifier is around -103.75 dB and for the logarithmic amplifier, it is around -112 dB. The SNR for the linear

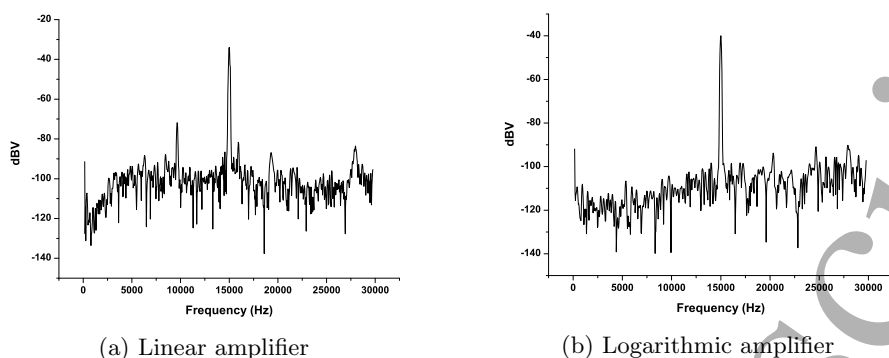


Figure 6: Spectrum of the output signal from (a) Linear amplifier, (b) Logarithmic Amplifier

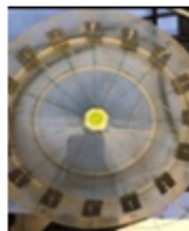
amplifier circuit is calculated to be 69.78 dB, whereas for the logarithmic amplifier it is 72.03 dB, thereby showing an improvement.

2.6. Test Phantoms

2.6.1. Non-biological and biological Phantoms. A circular tank made of plastic, 11 cm in radius, is filled with saline solution. Sixteen stainless steel electrodes, each of 1 cm in width and 4 cm in height, are attached to the inner surface of the tank. The electrodes are connected to the data acquisition system through a 16 pin flat ribbon cable. For non-biological phantom, non conducting objects of radius 0.25 cm and 0.5 cm are introduced at different positions in the tank (figure 7a). Biological phantom is designed with a cucumber in the saline tank (figure 7b).



(a) Non-biological



(b) Biological

Figure 7: Actual images of (a) non-biological phantom with non conducting object of 0.25cm radius , (b) biological phantom with cucumber of radius 1.15cm

2.6.2. Mini EIT sensor design for cell imaging applications. A mini EIT sensor consisting of sixteen planar electrodes fabricated on a double sided PCB is developed for cell imaging applications. The exposed copper is electroplated with gold for bio-compatibility. The width of each electrode is 0.5 mm. A circular well made of rubber with diameter of 10 mm is mounted on the mini EIT sensor and filled with the phosphate buffer solution (PBS) of concentration 10 mM. PBS is selected since it is used as the cell culture medium (Sun et al. 2009). A small object made of plastic

with 0.5 mm diameter is used as the in-homogeneity in the PBS solution as shown in figure 8.

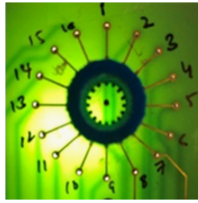


Figure 8: Mini EIT sensor

2.7. Image Reconstruction

Images are reconstructed using EIDORS, which is a MATLAB based open source software (Adler and Lionheart 2006). A forward model is created in EIDORS using a finite element method (FEM) containing 1024 elements. Inverse model is created for difference imaging where two sets of data at two different time intervals are used. The LabVIEW VI acquires the data and calculates the peak to peak voltages. In case of both the linear and the logarithmic amplifier based system, these voltages are directly fed to the reconstruction software as input data. In this paper, we have used one-step Gauss Newton linear difference solver from EIDORS toolbox (Polydorides and Lionheart 2002) for the reconstruction.

3. Results

SNR for the two EIT systems based on linear and logarithmic amplifier was calculated. Non-biological phantom was designed to compare the minimum size detectable by both the systems and biological phantom was used to find the minimum detectable change in conductivity.

Images obtained are quantitatively analyzed using parameters like Resolution (RES) and Contrast to noise Ratio (CNR) as defined below:

Resolution (RES) is defined as the ratio of the Area (in pixels) of the reconstructed image in the region of interest (ROI) to that of the total area of the entire reconstructed medium. ROI is defined as one-fourth amplitude set (Yasin et al., 2011). The smaller the value of RES, the better is the spatial resolution.

Contrast-to-Noise Ratio (CNR) is defined as the ratio of the difference between the average conductivity of in-homogeneity in the ROI and the average conductivity of the background, to that of the weighted average of the standard deviations of the conductivity values in the in-homogeneity region and the background region (Bera and Nagaraju, 2012). The higher the CNR, the better is the contrast recovery.

Experiments were also performed on the mini EIT sensor.

3.1. SNR

For SNR measurement, the sequence proposed by Gagnon (Gagnon et al., 2010) has been used. SNR is calculated as the ratio of mean of the signal on each channel to

that of the standard deviation on each channel.

$$SNR_i = \frac{[\bar{v}]_i}{SD_i} \quad (10)$$

where $[\bar{v}]_i$ is the mean value of the signal on i^{th} channel and SD_i is the standard deviation of multiple measurements on i^{th} channel. The measurements were carried for the homogenous tank filled with the saline solution having conductivity of 0.6 S m^{-1} . Stimulation current of 1 mA was applied to the electrodes and hundred frames of data were acquired. The SNR plot for the linear and the logarithmic amplifier based systems is shown in figure 9.

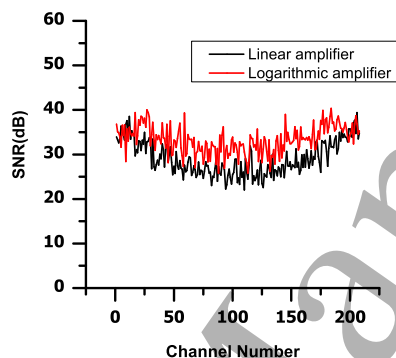


Figure 9: Plot for Signal to noise ratio (SNR) vs channel number for the linear amplifier and the logarithmic amplifier based EIT systems

For the linear amplifier based system, SNR ranges from 22 dB to 39.3 dB with an average SNR of 29 dB, whereas for the logarithmic amplifier based system, it ranges from 25.8 dB to 40.5 dB with an average of 33 dB as shown in figure 9. For channels opposite to the current injected ones, there is a 17 % increase in SNR of the EIT system with logarithmic amplifier. Overall, there is an improvement in the average SNR of the system by 4 dB.

3.2. Non-biological Phantom results

Small non-conducting objects of radius 0.25 cm and 0.5 cm were introduced at different positions in the saline filled tank having conductivity of 0.6 S m^{-1} . Current of 1 mA with 5 kHz frequency was injected through the electrodes. Data was acquired at a sampling frequency of 48 kS/s (Maximum sampling frequency of NI USB6008). The EIT data of linear and logarithmic amplifier based system is shown in figure 10a and the expanded view for single channel data is shown in figure 10b.

For single channel acquisition, data with the linear amplifier ranges from 0.7 V to 4.5 V, whereas with the logarithmic amplifier, it ranges from 0.66 V to 1.59 V. As expected, in case of the logarithmic amplifier based system, the range of data is reduced. Figure 11a and 11b shows the reconstructed images for targets of radius 0.25 cm and 0.5 cm kept at different positions.

The color-bar in the reconstruction shows relative change of local conductivity which is a non-dimensional quantity, wherein, red color represents higher conductivity regions and blue color represents lower conductivity regions. It is observed that with

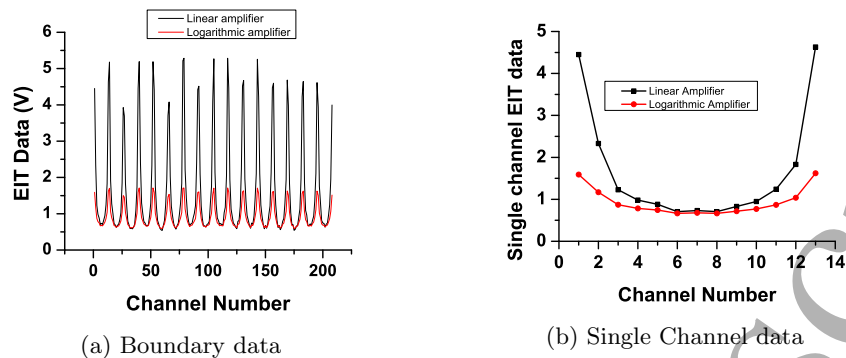


Figure 10: Plots showing (a) Boundary data, (b) single channel data, for logarithmic and linear amplifier based EIT systems

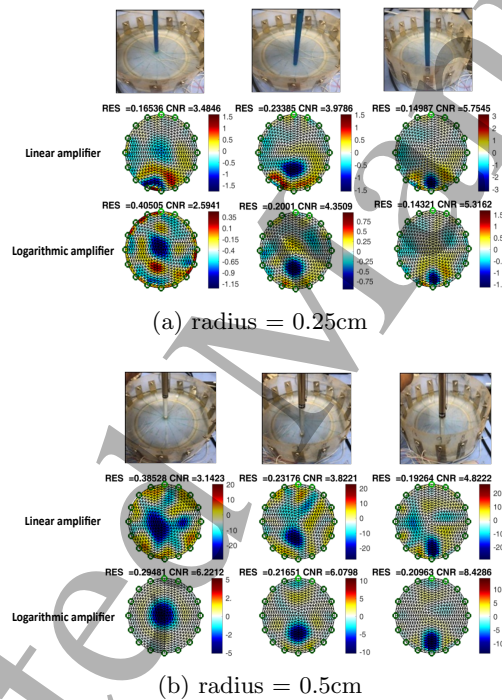


Figure 11: Reconstructed images using linear amplifier and logarithmic amplifier based system for target of radius (a) 0.25cm, (b) 0.5cm

the logarithmic amplifier, the target of radius 0.25 cm kept at the center is detected, whereas it is not detected by the linear amplifier based system. The values for RES as well as CNR for images are also shown in figure 11. It is observed that with the logarithmic amplifier based system, both RES and CNR are improved especially for anomalies kept at the center and middle, however, towards the periphery both systems have similar results.

3.3. Biological Phantom results

For small conductivity contrasts, experiments were performed using biological phantom with cucumber in the saline solution. The conductivity of the cucumber was calculated using an LCR meter. It was found to be 0.34 mS cm^{-1} at 5 kHz frequency. The conductivity ' σ ' of the saline solution was varied from 0.1 mS cm^{-1} to 0.5 mS cm^{-1} . Cucumber of size 2.3 cm in diameter was kept at different positions in the saline filled tank. Current of 1 mA with 5 kHz frequency was injected through the electrodes. Data was acquired for the logarithmic amplifier based EIT system and linear amplifier based system as the background conductivity ' σ ' was varied. Figure 12 shows the reconstructed images along with the color-bar showing relative change of local conductivity. The color bar for images obtained by the logarithmic amplifier based system shows smaller scale due to the smaller dynamic range of the logarithmic data.

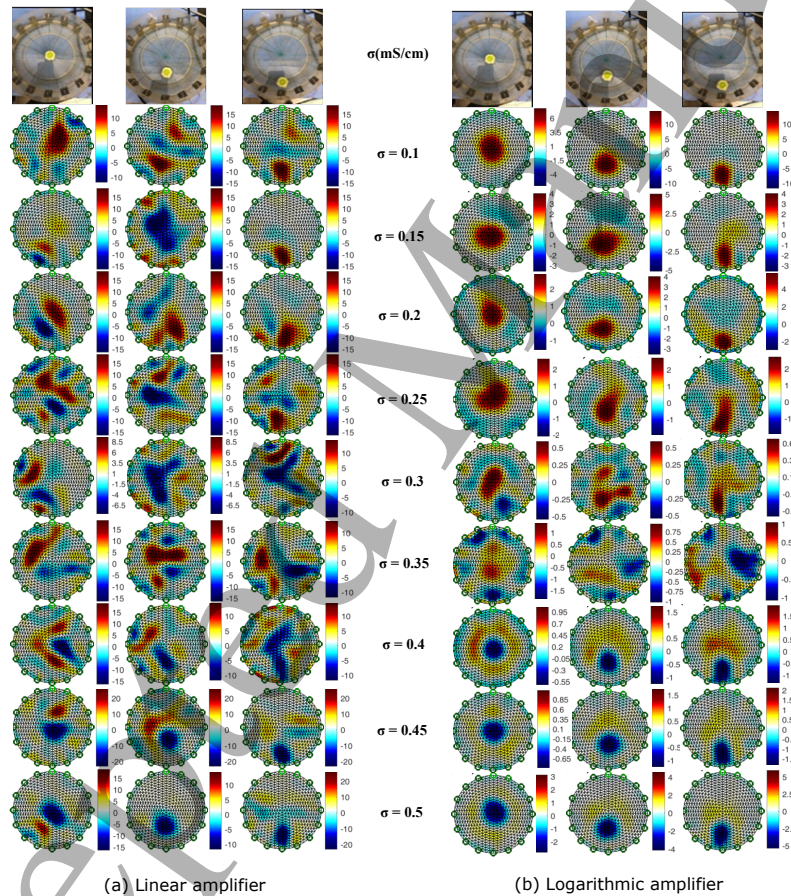


Figure 12: Reconstructed images of cucumber at different positions for varied background conductivity using (a) linear amplifier based system, (b) logarithmic amplifier based system

From figure 12, it is observed that with the linear amplifier, cucumber kept near electrodes is detected when the background conductivity is equal to or less than 0.25

mS cm⁻¹ or if it is greater than or equal to 0.45 mS cm⁻¹. Towards the center, it is detected when the background conductivity is less than 0.1 mS cm⁻¹ or greater than 0.45 mS cm⁻¹. For anomalies towards the electrodes, the minimum change in conductivity that the linear amplifier based system can detect is 32 % and for anomalies at the center, it is 70 %.

Logarithmic amplifier based system detects the anomaly near electrodes when the background conductivity is less than or equal to 0.3 mS cm⁻¹ or if it greater than or equal to 0.4 mS cm⁻¹. It detects anomaly at other positions when the background conductivity is less than or equal to 0.25 mS cm⁻¹ or if it greater than or equal to 0.4 mS cm⁻¹. The minimum change in conductivity detectable is 11 % for the anomalies near electrodes and 17.6 % at other positions. Overall, the logarithmic amplifier increases the sensitivity of the system to very small conductivity changes.

3.4. Mini EIT sensor results

A non-conducting object, made of plastic of diameter 0.5 mm, was introduced at different positions in the circular well, containing PBS solution as shown in figure 13. Current of 1 mA with 5 kHz frequency, was injected through the electrodes. Reconstructed images were compared for both logarithmic amplifier based system and linear amplifier based system. From the images shown in figure 13, it is observed

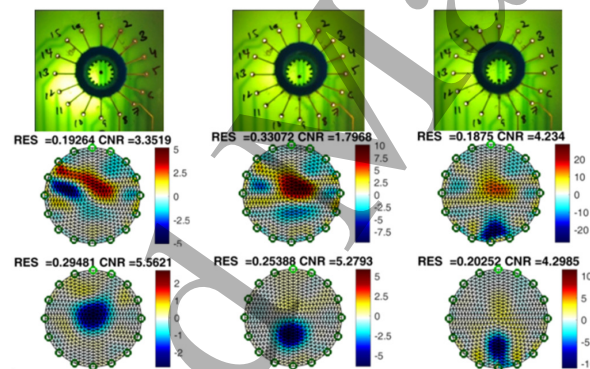


Figure 13: 1st row: Actual image of the mini sensor phantom, 2nd row: Reconstructed Images using linear amplifier, 3rd row: Reconstructed images using logarithmic amplifier

that the logarithmic amplifier based system can detect a small target of radius 0.5 mm even at the center of the well, which is not detected by a linear amplifier based system. RES and CNR of the images are also improved as shown in the images.

4. Discussion

This paper deals with the design of a signal conditioning circuit using a logarithmic amplifier, to improve the spatial resolution of a low-cost EIT system. In the present study, we have compared the performance of the logarithmic amplifier based EIT system and the linear amplifier based system when a low resolution ADC is used for data acquisition. Being a non-linear amplifier, logarithmic amplifier is said to improve

REFERENCES

13

the signal to noise ratio and the same is validated with the spectrum analysis of the output signal obtained from both amplifiers. The output spectrum of the logarithmic amplifier showed improvement of around 2 dB in the signal-to-noise ratio.

Various parameters of the EIT systems based on the logarithmic and the linear amplifiers were compared. Overall, there is an improvement of 4 dB in the average SNR of the EIT system using a logarithmic amplifier. Specifically, for the channels opposite to the current injecting electrodes, a 17 % improvement in the SNR was observed. For channels closer to the current injecting electrodes, there is no significant change in the SNR. This could be because these channels have high signal strength.

Reconstruction images further indicate that the logarithmic amplifier based EIT system can detect small size targets of radius as low as 0.25 cm in a tank of radius 11cm, whereas the linear amplifier based system could not detect targets of radius less than 0.5 cm. Logarithmic amplification also resulted in better resolution and contrast to noise ratio especially towards the center where the sensitivity is very low. Experiments performed with the biological phantom using a cucumber in the saline filled tank show that the minimum change in conductivity detected by the logarithmic amplifier based EIT system, for the anomalies towards the center is 17.6 %, whereas it is 70 % for the linear amplifier based system. For anomalies near the electrodes, it is 11 % and 32 % respectively. The logarithmic amplifier based EIT system also showed improvement in the resolution and contrast-to-noise ratio of the images obtained with the mini EIT sensor.

Though the logarithmic amplifier based EIT system shows an improvement over the linear amplifier based system we need to consider and work on overcoming its limitations as well. As explained in section 2.2, the logarithmic amplifier is not able to distinguish between EIT signals having higher signal strength because it compresses larger values. The strength of an EIT signal is influenced by the magnitude of current injected as well as the conductivity contrast (Gaggero 2011). Increasing the current or the conductivity contrast will increase the signal strength. Applications, which use high stimulation currents or have large conductivity contrast result in high signal strength. Under such circumstances, the use of logarithmic amplifiers might not be advantageous.

The present design of the logarithmic amplifier can cover the input signals ranging from 10 mV to 1 V. Further work on commercial off the shelf components to implement cascaded log amplifiers is being carried out to increase the input range.

5. Conclusion

The results indicate that the signal conditioning circuit using a logarithmic amplifier improves the SNR as well as the spatial resolution of a low-cost EIT system realized using a low resolution ADC. Further work is needed to optimize the design, so that it can cover a large input range. Logarithmic amplifier based systems will be advantageous mainly for the signals having low signal strength.

References

Adler, Andy, Bartłomiej Grychtol, and Richard Bayford (2015). *Why is EIT so hard, and what are we doing about it?* DOI: 10.1088/0967-3334/36/6/1067.

REFERENCES

14

- Adler, Andy and William R.B. Lionheart (2006). "Uses and abuses of EIDORS: An extensible software base for EIT". In: *Physiological Measurement*. Vol. 27. 5. DOI: 10.1088/0967-3334/27/5/S03.
- Barber, D. C. (2003). "Electrical impedance tomography". In: *Biomedical Imaging*. ISBN: 9780203491409. DOI: 10.2174/157339809788190002.
- Bera, Tushar Kanti and Nagaraju Jampana (2010). "A multifrequency constant current source suitable for Electrical Impedance Tomography (EIT)". In: *International Conference on Systems in Medicine and Biology, ICSMB 2010 - Proceedings*. ISBN: 9781612840383. DOI: 10.1109/ICSMB.2010.5735387.
- Bera, Tushar Kanti and J. Nagaraju (2009). "Studying the boundary data profile of a practical phantom for medical electrical impedance tomography with different electrode geometries". In: *IFMBE Proceedings*. ISBN: 9783642038785. DOI: 10.1007/978-3-642-03879-2-258.
- "1. Proceedings of the 20th International Conference on Biomedical Applications of EIT" (2019). In: ed. by Alistair Boyle et al. UCL, London, UK. DOI: 10.5281/zenodo.2691705. URL: <https://eit2019.co.uk/eit2019.pdf>.
- Brown, B. H. (2003). *Electrical impedance tomography (EIT): A review*. DOI: 10.1080/0309190021000059687.
- Chen, Chi Hau (1969). "Signal-to-Noise Ratios in Logarithmic Amplifiers". In: *Proceedings of the IEEE* 57.9, pp. 1667-1668. ISSN: 15582256. DOI: 10.1109/PROC.1969.7359.
- Gaggero, Pascal Olivier (2011). "Miniaturization and Distinguishability Limits of Electrical Impedance Tomography for Biomedical Application". In: *PhD Thesis Universite de Neuchâtel* June, p. 272.
- Holder, David S. (2004). *Part 1 of Electrical Impedance Tomography: Methods, History and Applications*. ISBN: 0750309520.
- Khan, Talha Ali and Sai Ho Ling (2019). *Review on electrical impedance tomography: Artificial intelligence methods and its applications*. DOI: 10.3390/a12050088.
- Martin, Sébastien and Charles T.M. Choi (2017). "A Post-Processing Method for Three-Dimensional Electrical Impedance Tomography". In: *Scientific Reports* 7.1. ISSN: 20452322. DOI: 10.1038/s41598-017-07727-2.
- Oljaca, Miro and Bonnie Baker (2009). "How the voltage reference affects ADC performance, Part 3". In: *Analog Applications*.
- Polydorides, Nick and William R.B. Lionheart (2002). "A Matlab toolkit for three-dimensional electrical impedance tomography: A contribution to the Electrical Impedance and Diffuse Optical Reconstruction Software project". In: *Measurement Science and Technology*. ISSN: 09570233. DOI: 10.1088/0957-0233/13/12/310.
- Rafiei-Naeini, Mandana, P. Wright, and H. McCann (2007). "Low-noise measurement for electrical impedance tomography". In: *IFMBE Proceedings*. Vol. 17 IFMBE. DOI: 10.1007/978-3-540-73841-1_85.
- Ranade, Nanda V. and Damayanti C. Gharpure (2019). "Enhancing sharp features by locally relaxing regularization for reconstructed images in electrical impedance tomography". In: *Journal of Electrical Bioimpedance* 10.1. ISSN: 18915469. DOI: 10.2478/joeb-2019-0002.
- Reynolds, Walter E (1965). *THE USE OF A LOGARITHMIC AMPLIFIER IN DATA PROCESSING OF ANALOG SIGNALS*. Tech. rep. URL: <https://profiles.nlm.nih.gov/ps/access/bbgcwj.pdf>.

REFERENCES

15

- 1
2
3
4
5 Sun, Tao et al. (2009). "Single cell imaging using electrical impedance tomography".
6 In: *4th IEEE International Conference on Nano/Micro Engineered and Molecular*
7 *Systems, NEMS 2009*. ISBN: 9781424446308. DOI: 10.1109/NEMS.2009.5068710.
8 Takhti, Mohammad, Yueh Ching Teng, and Kofi Odame (2018). "A 10 MHz Read-
9 Out Chain for Electrical Impedance Tomography". In: *IEEE Transactions on*
10 *Biomedical Circuits and Systems*. ISSN: 19324545. DOI: 10.1109/TBCAS.2017.
11 2778288.
12 Verma, M., D. C. Gharpure, and V. G. Wagh (2019). "Pre-processing of data using
13 logarithmic transformation to improve the spatial resolution of an EIT system
14 for biomedical applications". In: *Journal of Physics: Conference Series*. DOI: 10.
15 1088/1742-6596/1272/1/012021.
16 Wang, Jing, Bo Han, and Wei Wang (2019). "Elastic-net regularization for nonlinear
17 electrical impedance tomography with a splitting approach". In: *Applicable*
18 *Analysis* 98.12. ISSN: 1563504X. DOI: 10.1080/00036811.2018.1451644.
19 Xu, Yanbin, Bing Han, and Feng Dong (June 2018). "A new regularization algorithm
20 based on the neighborhood method for electrical impedance tomography". In:
21 *Measurement Science and Technology* 29.8. ISSN: 13616501. DOI: 10.1088/1361-
22 6501/aac8b6.
23 Yin, Xipeng et al. (2018). "A micro EIT sensor for real-time and non-destructive
24 3-d cultivated cell imaging". In: *IEEE Sensors Journal*. ISSN: 1530437X. DOI:
25 10.1109/JSEN.2018.2834509.
26 Yu, Chenglong et al. (2014). "An effective measured data preprocessing method in
27 electrical impedance tomography". In: *Scientific World Journal*. ISSN: 1537744X.
28 DOI: 10.1155/2014/208765.
29
30
31
32
33
34
35
36
37
38
39
40
41
42
43
44
45
46
47
48
49
50
51
52
53
54
55
56
57
58
59
60